Magnetic exchange interactions in Co-based II-VI diluted magnetic semiconductors: $Zn_{1-x}Co_xS$

T. M. Giebultowicz
Department of Physics, University of Notre Dame, Notre Dame, Indiana 46556
and National Institute of Standards and Technology, Gaithersburg, Maryland 20899

P. Klosowski
Department of Physics, University of Notre Dame, Notre Dame, Indiana 46556

J. J. Rhyne and T. J. Udovic
National Institute of Standards and Technology, Gaithersburg, Maryland 20899

J. K. Furdyna and W. Giriat*
Department of Physics, University of Notre Dame, Notre Dame, Indiana 46556
(Received 31 July 1989)

The exchange parameter J_{NN} for nearest-neighbor (NN) Co^{2+} ions in a new II-VI diluted magnetic semiconductor system $Zn_{1-x}Co_xS$ has been directly determined using inelastic-neutron-scattering techniques. The Co^{2+} ions in the system have a magnetic ground state with quenched orbital moment, so that the Co-Co interaction can be described, to a very good approximation, as a Heisenberg exchange between two $S=\frac{3}{2}$ spins. Inelastic-scattering spectra obtained from polycrystalline samples with $x=0.01-0.06$ reveal distinct maxima corresponding to transitions between the energy levels of isolated NN Co-Co pairs. The energy of the first excited level $E=2J_{NN}$ has been found to be $E=8.19\pm0.05$ meV, which yields $J_{NN}/k_B=47.5\pm0.6$ K, in good agreement with the result obtained from recent magnetic-susceptibility studies. The observed sequence of the excitation energies shows a slight deviation from the Landé interval rule, indicating biquadratic effects in the Co-Co exchange.

I. INTRODUCTION

We report the first direct measurements of the antiferromagnetic (AF) exchange constant J_{NN} between the nearest-neighbor (NN) Co ions in $Zn_{1-x}Co_xS$ using inelastic-neutron-scattering methods. $Zn_{1-x}Co_xS$ belongs to the family of diluted magnetic semiconductors (DMS), or semimagnetic semiconductors (SMSC), i.e., semiconducting alloys whose lattice is made up in part of substitutional magnetic ions (for reviews on DMS, see, e.g., Refs. 1 and 2). The investigation of basic magnetic exchange interactions in this novel class of materials continues to receive a great deal of attention of both experimentalists and theorists. In the last few years, a number of studies dedicated to this problem have been done on various II-VI, II-V, and IV-VI DMS alloys containing transition-metal ions[3-5] (mainly Mn) as well as rare-earth ions[6] (Gd and Eu). By far, the most extensively investigated group of such systems has been the $A^{II}_{1-x}Mn_xB^{VI}$ alloy series (where A^{II}=Zn, Cd, or Hg, and B^{VI}=S, Se, or Te). Experimental measurements of the exchange parameters in these materials have been made using a wide variety of experimental techniques,[3] and the J_{NN} values have been already determined for all members of the group which can be obtained in stable tetrahedral crystallographic forms.[7]

A remarkable achievement in the recent past has been the work of Larson *et al.*,[4] who formulated an *ab initio* theory providing a comprehensive description of the electronic band structure and the Mn-Mn exchange in the $A^{II}_{1-x}Mn_xB^{VI}$ alloy series. Their results made it possible to determine the hierarchy of the mechanisms constituting this interaction, and to prove that the overwhelming contribution arises from two-hole processes (i.e., from superexchange effects mediated by the anions), contrary to many previous opinions that the dominant role was played by one-hole–one-electron processes (i.e., the Bloembergen-Rowland exchange mechanism). Also, the theory of Larson *et al.* explains the chemical trends in the interaction within this alloy group.

In constrast to our present understanding of the $A^{II}_{1-x}Mn_xB^{VI}$ compounds, very little is still known about the exchange phenomena in II-VI DMS alloys containing transition-metal atoms other than Mn. One general conclusion[8] which can be drawn from the calculations of Larson *et al.* is that the short-range AF superexchange mechanism is likely to be dominant in all $A^{II}_{1-x}T_xB^{VI}$ alloys with $3d$ transition-metal elements T, so that no dramatic qualitative changes (e.g., a transition to ferromagnetism) can be expected in the case of such systems. On the other hand, the replacement of Mn^{2+} by ions with different electronic configurations may lead to significant changes in the interaction strength, or in the chemical trends within a given alloy family based on the

same magnetic ion. However, there is a lack of measured data from non-Mn-based systems which might shed light on these questions. Progress in the experimental studies of these materials has been limited primarily due to the lack of good quality crystals with sufficiently high concentration of the magnetic component. The incorporation of most transition elements into the II-VI lattices appeared to be a difficult problem that could not be readily solved by adapting the techniques used for the growth of $A^{II}_{1-x}Mn_xB^{VI}$ systems. It should be noted that the solubility of Mn in II-VI compounds is exceptionally high, up to 50–75 %. In recent years, the only success in this field has been the preparation of several new Fe-based II-VI DMS alloys.[9] Unfortunately, experimental study of the Fe-Fe exchange in these compounds is particularly difficult because of the spin-orbit coupling effects on the Fe^{2+} ion which greatly complicate the interpretation of measured data. Although much effort has been recently made to extract the Fe-Fe interaction parameters from magnetization and specific-heat data for $Zn_{1-x}Fe_xSe$, $Cd_{1-x}Fe_xSe$, and $Cd_{1-x}Fe_xTe$ by comparing those characteristics with numerically calculated theoretical curves[10] (taking into account all relevant effects), the J_{NN} values obtained by this method are not sufficiently accurate for a detailed quantitative analysis.

One of the latest achievements in the technology of II-VI DMS materials has been the preparation of an entirely new line of alloys based on cobalt. These systems offer excellent opportunities for broadening our insight into the magnetic exchange phenomena in this class of compounds. Because the orbital moment of Co^{2+} in II-VI lattices is quenched by the crystal field, the ions are effectively in S states, thus enabling the study of Co-Co exchange in a relatively straightforward way. The first information about this interaction has been obtained from magnetization and magnetoreflectivity studies of epitaxially grown $Zn_{1-x}Co_xSe$ films,[11(a)] and more recently, from Raman scattering studies of $Cd_{1-x}Co_xSe$,[11(b)] and from magnetic-susceptibility studies of $Zn_{1-x}Co_xS$ and $Zn_{1-x}Co_xSe$.[12] The measurements have revealed that the strength of the AF interactions in these systems is several times larger than in their Mn-based counterparts. More surprisingly, the data reported in Ref. 12 indicate stronger interactions in $Zn_{1-x}Co_xSe$ than in $Zn_{1-x}Co_xS$. Such behavior is in striking contrast to the regularity observed in the $A^{II}_{1-x}Mn_xB^{VI}$ alloys, in which the interaction strength always decreases with increasing atomic number of the B^{VI} anion.

The findings of magnetic-susceptibility studies have to be confirmed by more direct measurements of the exchange parameters. The results of experiments on $Zn_{1-x}Co_xS$ which we report in this paper show that inelastic neutron scattering offers an excellent tool for this purpose. The measurements have made it possible to establish that the nearest-neighbor exchange parameter in the system $J_{NN}/k_B=(47.5\pm0.6)$ K, which is, indeed, almost three times higher than for $Zn_{1-x}Mn_xS$.[13] It should be noted that the accuracy of this determination ($\Delta J/J$) is decidedly better than in any previous measurement of J_{NN} in DMS materials.

II. THEORETICAL BACKGROUND

A. Excitation spectrum of Co-Co pairs in $Zn_{1-x}Co_xS$

$Zn_{1-x}Co_xS$ crystallizes in the zinc-blende (cubic) structure, which is one of the two commonly occurring crystallographic phases of pure ZnS (the other being the hexagonal wurtzite phase). In both structures the cations occupy positions inside tetrahedra formed by four nearest-neighbor anions. A free Co^{2+} ion ($3d^7$ configuration) has a spin number $S=\frac{3}{2}$ and orbital momentum $L=3$. In a tetrahedral crystal field, the ground state of the free ion (^4F) is split into an orbital singlet ($^4A_2$) and two higher-lying orbital triplets [$^4T_2$ and $^4T_1$, see Fig. 1(a)]. The transition energies between the $^4A_2$ and the $^4T_2$ and $^4T_1$ states are $\sim$2750 cm^{-1} ($\sim$5400 K), and $\sim$6750 cm^{-1} ($\sim$9700 K), respectively, as found from infrared absorption studies[14] in Co-doped ZnS. The measurements have been done only for crystals of the wurtzite type; however, taking into consideration that the tetrahedral bond lengths and the nearest-neighbor configuration around a given Co^{2+} ion are almost identical in both structural forms of ZnS (the only difference is a slight trigonal distortion occurring in the wurtzite phase, which leads to an additional splitting of the $^4T_2$ and $^4T_1$ states), one can expect that there is no significant change in these values in the case of the zinc-blende crystals.

Because the ground state $^4A_2$ is an orbital singlet, the interaction between two NN Co ions can be treated, in the first approximation, as a Heisenberg-type exchange for a pair of $S_i=S_j=\frac{3}{2}$ spins described by the following Hamiltonian:

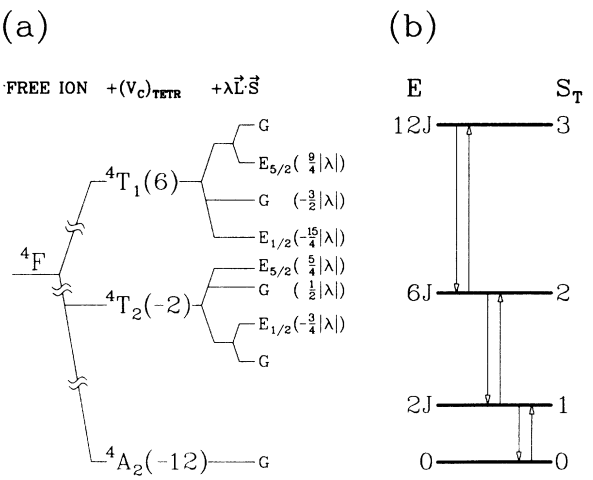

FIG. 1. (a) Energy-level diagram for a Co^{2+} ion in a tetrahedral crystal field (after Ref. 14). (b) Energy levels for a pair of $S=\frac{3}{2}$ spins; S_T is the total spin, and E is the energy of a given state. The arrows show the allowed transitions ($\Delta S=\pm1$) in inelastic-neutron-scattering processes.

$$\mathcal{H}=2J_{\mathrm{NN}}\mathbf{S}_i\cdot\mathbf{S}_j \ . \tag{1}$$

The eigenstates of Eq. (1) can be described in terms of the total spin $\mathbf{S}_T=\mathbf{S}_i+\mathbf{S}_j$, where S_T can take the values $S_T=0$, 1, 2, and 3. The energies of these states follow a Landé interval rule and are given by

$$E(S_T)=J_{\mathrm{NN}}[S_T(S_T+1)-S_i(S_i+1)-S_j(S_j+1)] \ . \tag{2}$$

Taking $E(S_T=0)$ as 0, the energies of the three excited states for a Co^{2+}-Co^{2+} pair can be written simply as $2J_{\mathrm{NN}}$, $6J_{\mathrm{NN}}$, and $12J_{\mathrm{NN}}$. Experimental measurements of these energies thus provide a straightforward way of determining the J_{NN} value.

In fact, the measured value[15] of the Landé g factor for Co^{2+} in ZnS appears to be considerably higher than the value expected for a spin-only state (2.248, as opposed to 2.002), which indicates that there is a certain amount of admixture from higher-lying states with $L\neq 0$ into the ground state, in spite of the large crystal-field splitting. Such mixing of states is a well-known effect in the theory of transition-metal ions in ligand fields and can be explained as a second-order perturbation process.[16,17] The spin-orbit coupling $\lambda\boldsymbol{L}\cdot\mathbf{S}$ that is introduced in this way may lead to a single-ion anisotropy, and to an anisotropy in the ion-ion exchange even in cases of ions with orbital singlet ground states. We would therefore consider to what extent this mechanism may affect the Co-Co excitation spectrum in the case presently investigated. Fortunately, the interaction between two magnetic ions in the presence of spin-orbit coupling has been widely discussed in the literature in the context of electron-paramagnetic-resonance (EPR) studies. Excitation spectra of pairs of ions with singlet and orbitally degenerate magnetic ground states have been also discussed in some recent neutron scattering works.[18,19]

Following Kanamori,[16] and Owen and Harris,[20] if the two ions have orbital singlet ground states, the anisotropic part of the interaction can be introduced into the spin Hamiltonian $\mathcal{H}$ in the form of two additional terms, so that

$$\mathcal{H}=2J\mathbf{S}_i\cdot\mathbf{S}_j+2D(3S_{iz}S_{jz}-\mathbf{S}_i\cdot\mathbf{S}_j)+2E(S_{ix}S_{jx}-S_{iy}S_{jy}) \ , \tag{3}$$

where the subscripts x,y,z denote the Cartesian components of the spin vectors, with the z axis directed along the line joining the ions. The second term in the equation represents the so-called pseudodipolar exchange. The magnitude of the D coefficient is of order

$$D\lesssim J\lambda^2/\Delta^2 \ , \tag{4}$$

where Δ is the crystal-field splitting; the fact that λ and Δ appear in Eq. (4) as squares can be understood if we keep in mind that the anisotropy arises as a second-order perturbation effect. The last term in Eq. (3) has to be added if the symmetry is lower than axial (which is the case in $Zn_{1-x}Co_xS$, where the NN pairs lie along [110]-type axes). Usually, E is of comparable magnitude or lower than D. If $J\gg D,E$, the system can still be described in terms of the total spin $\mathbf{S}_T=\mathbf{S}_i+\mathbf{S}_j$, with $S_T=0,1,\ldots,S_i+S_j$, and the energies of these spin multiplets $E(S_T)$ follow the Landé interval rule. Equation (3) can then be expressed as

$$\mathcal{H}=E(S_T)+D_S[S_z^2-\tfrac{1}{3}S_T(S_T+1)]+E_S(S_x^2-S_y^2) \ , \tag{5}$$

which describes the splitting of the states within a given S_T multiplet (the connection between D, E, and D_S, E_S coefficients is given in Ref. 21).

Although data for D and E are not available for $Zn_{1-x}Co_xS$, considering that the crystal-field splitting is $\Delta\approx 3750\ \mathrm{cm}^{-1}$, and the spin-orbit coupling coefficient for Co^{2+} is $\lambda=178\ \mathrm{cm}^{-1}$ (after Ref. 14), one can estimate that in this material $D\approx J/400$. This shows that the excitation spectrum of a Co-Co pair is indeed correctly given by Eq. (2), except for a weak splitting of the levels. Such a splitting might perhaps be detected by EPR measurements. However, taking into account that the value of J_{NN} in $Zn_{1-x}Co_xS$ is about 4 meV, and the typical resolution of neutron spectrometers in the relevant energy range is about 1 meV, one can expect that the splitting may manifest itself only as a slight broadening of the inelastic-neutron-scattering lines.

Considering that the crystal-field splitting Δ of Co^{2+} states in other tetrahedral II-VI compounds[14,22] is of the same order of magnitude as in ZnS, one can expect that a simple isotropic Heisenberg model with $S=\frac{3}{2}$ should provide a good description of the Co-Co interaction in all DMS systems from the $A^{\mathrm{II}}_{1-x}Co_xB^{\mathrm{VI}}$ family. It should be kept in mind, however, that the interaction between Co^{2+} ions may be far more complicated in systems with crystal-field symmetry other than tetrahedral (e.g., in $KCo_xMg_{1-x}F_3$, see Ref. 19, or in $Co_xMg_{1-x}O$, see Ref. 23).

B. Neutron scattering from isolated pairs of magnetic ions

While there exist several ways to obtain the energies of excited pair states from various macroscopic measurements (e.g., from specific heat,[24] or from the step-like behavior of high-field magnetization curves[25]), the most straightforward method of investigating these levels is neutron scattering. In inelastic-scattering processes, the neutron energy loss or gain is equal to the difference between two neighboring levels (the selection rules for neutron scattering permit $\Delta S_T=0,\pm 1$, see Ref. 26), thus providing a direct and accurate measure of J. This technique has been successfully used for studying the interactions in many diluted antiferromagnets[27,28] (including some of the $A^{\mathrm{II}}_{1-x}Mn_xB^{\mathrm{VI}}$ alloys[13,29]), as well as in organic molecules containing transition-metal ion complexes.[30] The theoretical background of the neutron scattering method is presented in detail in a review article by Furrer and Gudel.[26]

In zinc-blende DMS alloys, the magnetic ions are randomly distributed over a fcc cation sublattice. The probability that a given ion belongs to a particular cluster type[31] is $P_1=(1-x)^{12}$ for singlets, $P_2=12x(1-x)^{18}$ for NN pairs, and so on. For example, in a system with $x=0.05$, 54% of ions are singlets, 24% are members of NN pairs, 4% belong to triads, and the remainder to

larger clusters like quartets, quintets, etc. Because single Co^{2+} ions in II-VI compounds do not have excited levels with transition energies in the relevant range, and therefore do not contribute to inelastic magnetic neutron scattering, the pair scattering is the dominant magnetic inelastic effect in this alloy composition region. Nonetheless, the intensity of this scattering is still relatively weak, because the pairs constitute only a small fraction of the total number of atoms in the sample. The origin of the inelastic lines observed in the experiments should therefore be carefully investigated in order to avoid possible misinterpretations (e.g., phonon scattering may produce peaks of comparable intensity). Some of the experimental procedures that can be used for this purpose are briefly discussed below.

The simplest method of identifying the pair scattering maxima is based on the fact that the neutron energy change in this process does not depend on momentum transfer. In contrast, phonon scattering usually exhibits a pronounced dispersive behavior, so that the two effects can be easily distinguished by measuring the inelastic-scattering spectra at various Q-space points. The dispersionless character of pair scattering also presents an advantage in that the experiments can be done on polycrystalline or powder samples; single-crystal specimens are necessary only in the case of some special measurements, e.g., in studies of anisotropic exchange effects.

Another signature of magnetic pair scattering is its temperature behavior. Because in most magnetic solids the exchange parameters show no significant dependence on T, the temperature shift of the inelastic peak positions is usually negligibly small. However, there is a very characteristic temperature dependence in the scattering intensity: At low temperature ($T \ll J$) practically all pairs are in the lowest energy state $|0\rangle$, so that only the $|0\rangle \rightarrow |1\rangle$ transition is possible, and one observes a single maximum at $E = 2J$ [see Fig. 1(b)]. As the temperature is raised, the population of the excited levels gradually increases, giving rise to a $|1\rangle \rightarrow |2\rangle$ peak at $4J$, and other possible transition peaks at higher energies. At the same time, the first maximum *decreases* in intensity. This latter effect is again in sharp contrast to the behavior of phonon lines, the intensity of which normally increases with increasing T.

Although, as noted, the energy transfer in scattering from pairs is $\mathbf{Q}$ independent, the peak intensity does vary with $\mathbf{Q}$ due to an interference term in the scattering cross section. If we consider only the $\mathbf{Q}$-dependent terms, the cross section for a process involving a $|S_T\rangle \rightarrow |S_T'\rangle$ transition in a single crystal can be written as[26]

$$\frac{d^2\sigma}{d\Omega\, dE} \propto \frac{k'}{k} f^2(Q)\exp[-2W(Q)] \times \sum_{ij} \{1+(-1)^{S_T - S_T'}\cos[\mathbf{Q}\cdot(\mathbf{R}_i - \mathbf{R}_j)]\} , \quad (6)$$

where k and k' are the wave numbers of the incident and scattered neutrons, respectively, $f(Q)$ is the magnetic form factor, W is the Debye-Waller factor, $\mathbf{R}_i$ and $\mathbf{R}_j$ are the positions of the ions comprising the pair, and the sum runs over all pairs in the crystal. Due to the oscillating term

$$\cos[\mathbf{Q}\cdot(\mathbf{R}_i - \mathbf{R}_j)]$$

in the cross section, measurements of the scattering intensity versus Q yield direct information about the radius vector $\mathbf{R}_{ij}$ between the magnetic ions, thus enabling a precise identification of the cluster type. It should be noted that in many fcc antiferromagnets the dominant exchange interaction is between the next-nearest neighbors, and such pairs may also give rise to inelastic peaks. For powders or polycrystalline materials, Eq. (6) has to be averaged in Q space, which leads to

$$\left\langle \frac{d^2\sigma}{d\Omega\, dE} \right\rangle_Q \propto \frac{k'}{k} f^2(Q)\exp[-2W(Q)] \times \left[1+(-1)^{S_T - S_T'} \frac{\sin(QR)}{QR} \right] \quad (7)$$

where $R = |\mathbf{R}_i - \mathbf{R}_j|$. Although the oscillating character of the Q dependence for polycrystalline specimens is less pronounced than in the case of single crystals, it is sufficient to enable an identification of pair spectra in a fcc lattice.

Finally, a simple test of the pair scattering results can be done by comparing the intensity data from samples with different magnetic ion concentrations x. For instance, the number of NN pairs per unit volume in fcc alloys is proportional to $xP_2 = 12x^2(1-x)$[18], and the ratio of scattering intensities for two alloys with concentrations x' and x'' normalized to the sample volume will vary as

$$\frac{i(x')}{i(x'')} = \frac{(x')^2}{(x'')^2} \left[\frac{1-x'}{1-x''} \right]^{18} . \quad (8)$$

III. EXPERIMENT

A. Samples

Neutron scattering experiments have been done on three $Zn_{1-x}Co_xS$ samples with nominal Co concentrations $x = 0.06$, 0.05, and 0.01 (labeled, respectively, as Samples 1, 2, and 3). Sample 1 was grown by using a high-pressure inert gas furnace and consisted of two separate ingots with volumes approximately 4 cm^3. As indicated by the appearance of the cleaved surfaces and by neutron-diffraction tests, both ingots consisted of many randomly oriented single-crystal grains with sizes 1–5 mm. Because of the relatively weak scattering intensity for magnetic pairs, sample volumes as large as possible are desired. Thus we did not attempt to cut out single-crystal specimens, but used the ingots in their existing form and treated them as "rough polycrystals." The phase homogeneity of the material was checked by carrying out measurements on a powder neutron diffractometer, with the sample rotating during the measurement. As found from the diffraction patterns, the content of the wurtzite phase in the samples was lower than 0.5%. Samples 2 and 3, with volumes 5 and 3 cm^3, respectively, were prepared using ceramic techniques

from mixed ZnS and CoS fine powders. The mixture was pressed into pellets and sintered for 10 d at 1000 °C. The pellets were then ground and the procedure repeated. After 20 d of sintering, the material showed no observable CoS diffraction peaks, but the wurtzite phase content in the sintered samples was much higher (up to 5%) than in those obtained by the high-temperature method. However, such contamination is not particularly harmful in J_{NN} measurements because the parameter values in the two structures of $Zn_{1-x}Co_xS$ are expected to be very similar (due to almost identical anion-cation tetrahedral bond lengths in both crystallographic phases). Nevertheless, even in the case of a larger difference, a scattering component with 5% of the intensity of the main spectral peak will result in only a negligibly small shift of the line position.

B. Instruments

Inelastic-neutron-scattering measurements were carried out at the 20 MW research reactor at the National Institute of Standards and Technology (NIST) using two types of instruments: (i) a triple-axis crystal spectrometer (TAS), and (ii) a time-of-flight (TOF) spectrometer.

The TAS measurements were made using a (002) pyrolytic graphite (PG) monochromator and analyzer, and 40′ angular collimation throughout the instrument. The spectrometer was operated in a constant-Q mode, with the final energy fixed at 14.8 meV. A 2-in. PG filter was placed in front of the analyzer in order to eliminate the $\lambda/2$ component in the incident beam.

The TOF measurements were carried out on a spectrometer installed on the cold neutron source of the NIST reactor. A pulsed monochromatic incident neutron beam with $E_0=13.8$ meV was produced using a double PG monochromator, a PG filter, and a curved-blade Fermi chopper. The pulse length was approximately 7 μs. The sample was placed in the center of a wide circular counter bank (with radius 228 cm) consisting of 98 independent ^{3}He detectors, covering a scattering angle range from $2\theta=6°$ to 116°. The time-of-flight spectrum registered by each detector was stored in a separate memory location.

Unlike crystal spectrometers, TOF instruments cannot be operated in a constant-Q mode. A TOF measurement carried out with a single thin counter at angle 2θ corresponds to a curved scanning trajectory in Q,E space, and with a wide circular counter the effect observed for a given E-transfer corresponds to a broad Q-transfer range. Hence, the method is best suited for studying dispersionless phenomena. Multidetector banks offer certain advantages in this type of measurement, making it possible, in principle, to calculate the spectrum shape for a given constant value of Q_0. However, due to the low counting statistics in our measurements, we could only partially take advantage of that capability of the instrument: By summing the counts from various detector groups, we were able to obtain spectra corresponding to "low-," "intermediate-," or "high-Q" ranges.

C. Experimental results

The principal feature of the inelastic-scattering spectra obtained from all TAS and TOF measurements on Samples 1 and 2 at low temperatures is a strong maximum corresponding to neutron energy loss ~8.2 meV. Examples of the TAS data from Sample 2 obtained for several different momentum-transfer values Q are displayed in Fig. 2. As illustrated by the figure, the positions of the inelastic peaks show no shift within the whole Q range investigated, within the experimental error of ±0.0.4 meV. The integrated intensities of the maxima in Fig. 2 are plotted versus Q in Fig. 3, together with similar data for Sample 1. The solid curves in this figure are the theoretical dependences of the scattering intensity from nearest-neighbor (NN) and next-nearest-neighbor (NNN) pairs in polycrystalline $Zn_{1-x}Co_xS$ calculated using Eq. (7) and published $f(Q)$ data for the Co^{2+} ion.[32] The absence of any detectable shift with Q, and the good agreement of the measured intensity data with the upper curve in Fig. 3, clearly show that the observed maxima originate from magnetic scattering from NN Co-Co pairs.

Further evidence that the observed processs represents magnetic pair scattering is its dependence on temperature. An example of the data obtained from Sample 1 at various temperatures is shown in Fig. 4. At 10 K, the spectrum shows no distinct features other than the peak at $\Delta E=8.2$ meV. When the temperature is raised, the intensity of the peak visibly decreases, whereas another

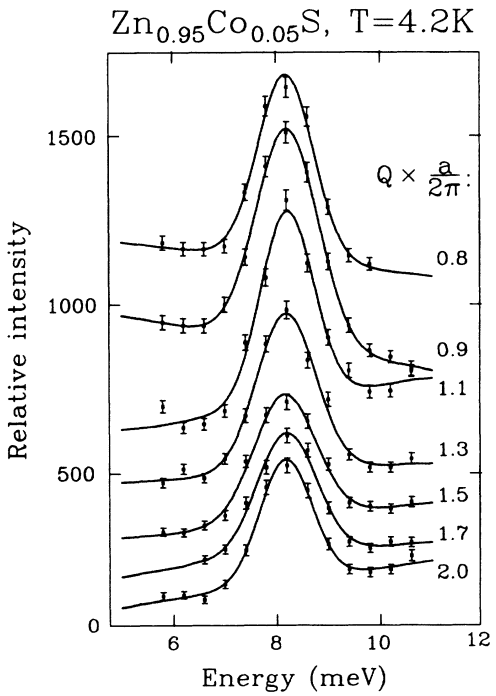

FIG. 2. The $|0\rangle \rightarrow |1\rangle$ pair transition peaks obtained from TAS measurements on $Zn_{0.95}Co_{0.05}S$ (Sample 2) at $T=4.2$ K for several different momentum transfers Q. The peaks are plotted on the same scale (and shifted upward for clarity) to illustrate the dispersionless character of the process.

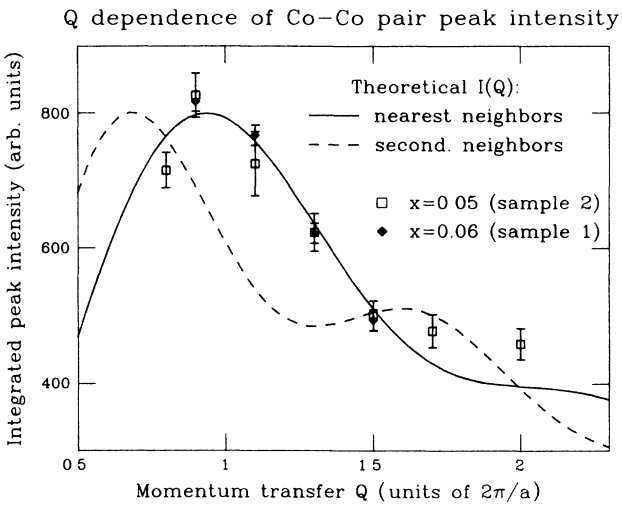

FIG. 3. The integrated intensities of the peaks shown in Fig. 2 plotted vs Q, together with similar data obtained from Sample 1. The solid and dashed lines are the theoretical integrated intensities calculated, respectively, for NN and NNN Co-Co pairs in $Zn_{1-x}Co_xS$ using Eq. (7).

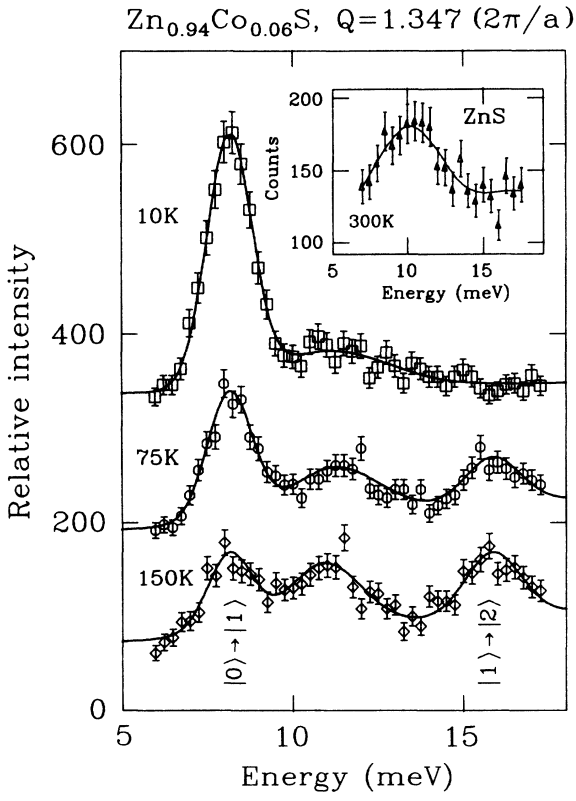

FIG. 4. Inelastic-scattering spectra obtained from TAS measurements on $Zn_{0.94}Co_{0.06}S$ (Sample 1) at various temperatures, showing the decrease of the intensity of the $|0\rangle \rightarrow |1\rangle$ transition peak, and the emergence of the $|1\rangle \rightarrow |2\rangle$ peak with increasing T (the spectra for 10 and 75 K are shifted upward for clarity). As shown in the inset, the maximum emerging at $E \approx 11$ meV is also seen in the data from pure ZnS, indicating that this effect arises from phonon scattering.

maxima gradually shows up near the double ΔE value, in total agreement with the expected behavior [see Fig. 1(b)]. In addition, the data also show a broad feature at ~ 11 meV which cannot be accounted for by the pair excitation mechanism. However, as illustrated by Fig. 5, the density of phonon states[33] in cubic ZnS exhibits a pronounced maximum at about the same energy region; the additional peak in the spectra can therefore be attributed to phonon scattering. Further confirmation of this interpretation was obtained from test measurements on a polycrystalline sample of pure ZnS, which indeed revealed a maximum of similar shape and location as that seen in the $Zn_{1-x}Co_xS$ spectra (see the inset in Fig. 4).

As expected, the maximum at 8.2 meV observed in experiments on Sample 3 (with $x=0.01$) was decidely weaker than in the case of the two other samples with higher Co concentrations, but still identifiable. The ratio of normalized scattering intensities from Samples 2 and 3 measured at identical conditions (see Fig. 6) was $i'/i''=14\pm2$, in reasonable agreement with the value of $i(0.05)/i(0.01)=11.9$ calculated from Eq. (8).

Examples of inelastic-scattering data from measurements on the TOF spectrometer are presented in Fig. 7. The right-hand panel of the figure shows the low-T spectrum obtained for Sample 1 by summing the contributions from all 98 detectors. The momentum-transfer range probed in the measurement (for neutron energy loss of 8.2 meV) extended from 0.95 to 3.6 Å^{-1}. The fact that averaging over such a broad Q range leaves the inelastic peak linewidth unchanged (essentially resolution limited) provides yet another proof for the dispersionless character of the observed process, and thus for its pair scattering nature.

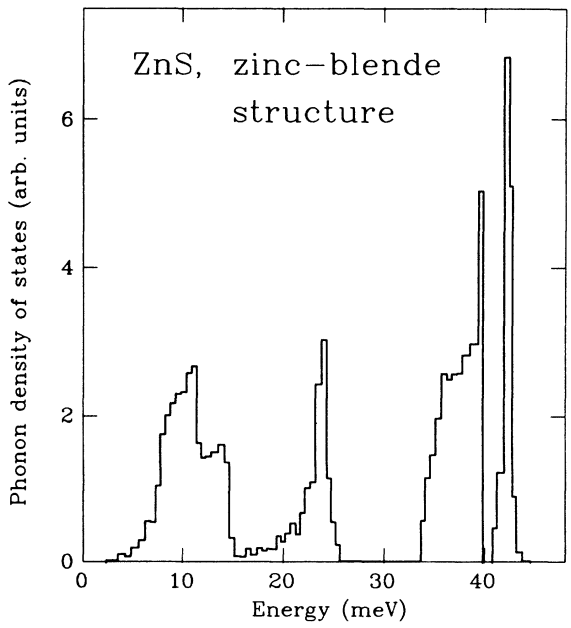

FIG. 5. The density of phonon states $D(\omega)$ for zinc-blende ZnS (after Ref. 33).

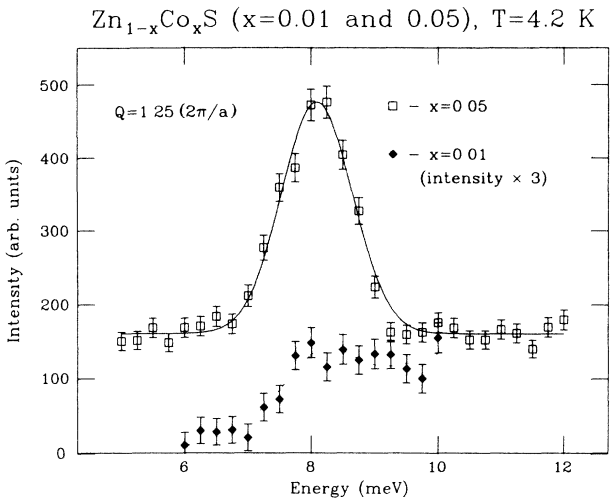

FIG. 6. The $|0\rangle \rightarrow |1\rangle$ pair transition peaks obtained from TAS measurements on Samples 2 ($x=0.05$) and 3($x=0.01$) carried out at identical conditions. The curve for Sample 3 has been shifted downward for clarity.

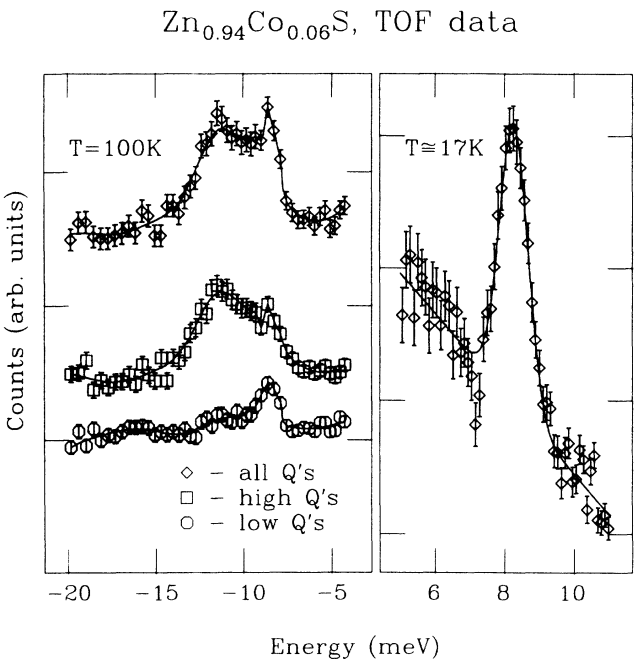

FIG. 7. Examples of inelastic TOF data for $Zn_{0.94}Co_{0.06}S$ (Sample 1). The right panel shows the neutron energy-loss side of the spectrum obtained at 17 K with a fitted Gaussian line shape. The left panel shows the energy-gain spectra at 100 K obtained by summing the counts from all detectors, as well as from the "high-Q" and the "low-Q" detectors (see text); the curves are guides for the eye.

As in the TAS measurements, the intensity of the peak at 8.2 meV was found to decrease when the temperature was increased to $T=100$ K. However, a more interesting part of the spectrum obtained in the latter measurement is its *energy gain* side (corresponding to $\Delta E<0$ in our notation), shown in the left panel of Fig. 7. The spectrum obtained by summing the contributions from all detectors

TABLE I. Summary of the $E(|0\rangle \rightarrow |1\rangle)$ data from various measurements.

Sample No. and x	Instrument type	Q (Å^{-1})	T (K)	Fitted E (mev)
Sample 1	TAS 2[a]	0.9	8.5	8.11±0.06
$x=0.06$	TAS 2	1.1	8.5	8.15±0.05
	TAS 2	1.3	8.5	8.11±0.06
	TAS 2	1.5	8.5	8.10±0.06
	TAS 9	1.35	10	8.18±0.03
	TAS 9	1.35	75	8.20±0.04
	TAS 9	1.35	150	8.15±0.07
	TOF	0.95–3.6	17	8.25±0.04
	TOF	0.95–3.6	100	8.30±0.06
Sample 2	TAS 6	0.8	4.2	8.21±0.03
$x=0.05$	TAS 6	0.9	4.2	8.23±0.03
	TAS 6	1.1	4.2	8.22±0.04
	TAS 6	1.3	4.2	8.20±0.03
	TAS 6	1.5	4.2	8.17±0.03
	TAS 6	1.7	4.2	8.20±0.03
	TAS 6	2.0	4.2	8.19±0.03
	TAS 9	1.25	6.0	8.13±0.05
	TOF	0.95–3.6	4.2	8.27±0.05
Sample 3	TAS 9	1.25	4.2	8.17±0.11
$x=0.01$				

[a]TAS 2, 6, and 9 refer to three different spectrometers used in the experiments.

shows a weak but well-resolved peak at ~ 8 meV, as well as a broad feature centered at ~ 11 meV. The latter effect is apparently produced by phonon scattering, as already identified in the case of TAS data, while the narrow line arises from pair scattering. Such an interpretation is confirmed by the two lower plots, which show the "low-Q" and the "high-Q" components of the total spectrum, obtained by summing the contributions from detectors covering the 2θ ranges from 6° to 60°, and from 60° to 116°, respectively. For neutron energy gain of 11 meV, these angle ranges correspond to Q ranges 0.9–3.1 Å^{-1} and 3.1–5.1 Å^{-1}, respectively. As indicated by these data, the broad maximum at about 11 meV arises primarily from processes involving high momentum transfers. This is, indeed, the expected behavior in the case of phonon scattering, considering that the cross section for the process is proportional to Q^2. In contrast, because magnetic scattering is damped at larger values of Q by the form factor $f(Q)$, the pair peak appears only in the low-Q data.

It should be noted that the process which gives rise to the magnetic peak is a transition from the first excited pair state $|1\rangle$ back to the ground state $|0\rangle$, not the $|0\rangle \rightarrow |1\rangle$ transition corresponding to all data previously shown, which involve neutron energy loss. Using the well-known optical terminology, the $|0\rangle \rightarrow |1\rangle$ and $|1\rangle \rightarrow |0\rangle$ scattering events can be referred to as "Stokes" and "anti-Stokes" processes, respectively. The occurrence of "anti-Stokes" maxima is, of course, fully predictable, considering the selection rules for inelastic scattering ($\Delta S = \pm 1$). However, the "anti-Stokes" process requires that the $|1\rangle$ state be populated, which explains why this maximum can be observed only at higher T.

The $|0\rangle \rightarrow |1\rangle$ peak positions ΔE obtained by fitting Gaussian line shapes to the results of various measurements on Samples 1–3 are listed in Table I. By calculating the weighted average of the data from all low-T runs (i.e., for $T \leq 17$ K) we obtain for the energy of the first excited level of NN Co-Co pairs in the $Zn_{1-x}Co_xS$ the value (8.19±0.05) meV.

It is important to note that in all cases (including the measurements at higher T) the maxima showed no significant broadening effects. The TOF measurements offered the best energy resolution: For energy loss of 8.2 meV, the calculated instrumental linewidth was $\Delta E = 0.85$ meV, and the linewidth obtained from fits to the low-T data was 0.96 meV, indicating an intrinsic width $\Delta E_i \lesssim 0.5$ meV. In the TAS measurements, where the instrumental resolution was 1.3–1.5 meV, no excess width was observed.

IV. DISCUSSION

The value of the exchange parameter $J_{NN} = \frac{1}{2}E(|0\rangle \rightarrow |1\rangle)$ obtained from our experiments is 4.10±0.03 meV, or 47.5±0.6 K in the commonly used J/k_B notation, which agrees well with the value of (47±6) K obtained from recent magnetic-susceptibility studies in $Zn_{1-x}Co_xS$.[12] Taking into account that the magnetic-susceptibility data contain contributions from other Co-Co pairs (NNN, NNNN, etc.), such good agreement between the two results points out that the NN coupling is the dominant antiferromagnetic interaction in the material. This conclusion is further supported by the absence of significant broadening effects in the spectra which could be expected from strong NNN or NNNN exchange coupling. As follows from the calculations of Larson, Hass, and Aggarwal,[31] who analyzed the effects of NNN and NNNN interactions on magnetization steps, in a system with $x = 0.05$ only about 13% of all pairs can be treated as isolated, while the remainder experience local exchange fields produced by these neighbors. Calculation of the effective broadening of pair levels due to such interactions is relatively straightforward only for high external magnetic fields (when all loosely coupled spins are oriented in the same direction), but presents a nontrivial problem if $H = 0$, which is normally the case in neutron scattering experiments. Nonetheless, a rough estimate of the peak broadening can be obtained by considering an NN pair $\mathbf{S}_1, \mathbf{S}_2$ with a weakly coupled third spin $\mathbf{S}_3$, and putting $J_{13} = J_{23} = J' \ll J_{NN}$. Taking the expression for energy eigenvalues of symmetric three-spin clusters,[26] one can readily show that the inclusion of the third spin leads to a splitting of the $E = 2J_{NN}$ transition peak into two lines, $8J'$ apart. Hence, a conservative estimate of the level broadening $\Delta E/E$ in a real system can be taken as J'/J_{NN}, where J' is a "mean" parameter for the NNN and NNNN interactions. The fact that we observe $(\Delta E/E) \lesssim 0.05$ indicates that the ratios of J_{NNN}/J_{NN}, J_{NNNN}/J_{NN} in $Zn_{1-x}Co_xS$ are comparable or lower than in materials from the Mn-based series.[4,31,34]

These findings are fully consistent with the general conclusion drawn from the theory of Larson *et al.* that the nearest-neighbor superexchange mechanism should play a dominant role in all $A^{II}_{1-x}T_xB^{VI}$ systems.[4,8] However, it is not yet clear why the exchange parameter for the Co-Co interaction in $Zn_{1-x}Co_xS$ is three times larger than for the Mn-Mn interaction in $Zn_{1-x}Mn_xS$. In addition to that, not only the magnitude of the interaction is surprising: As noted in Sec. I, magnetic-susceptibility data[12] indicate that J_{NN} in $Zn_{1-x}Co_xSe$ is even higher (54±8 K) than in $Zn_{1-x}Co_xS$, the ratio of the two parameters being 0.9±0.25. This value strongly contrasts with the chemical trends observed in the Mn-based family (the corresponding ratio of J_{NN}'s for $Zn_{1-x}Mn_xS$ and $Zn_{1-x}Mn_xSe$ is ~ 1.32, and for $Cd_{1-x}Mn_xS$ and $Cd_{1-x}Mn_xSe$ is ~ 1.27, based on the data from Refs. 13, 31, and 35), and cannot be understood on the grounds of the existing theory. Because the error margin in the magnetic-susceptibility data is rather large, it should be mentioned that the preliminary inelastic-neutron-scattering measurements already made on two $Zn_{1-x}Co_xSe$ samples[36] have yielded $J_{NN} = (50 \pm 1)$ K, thus confirming that such an anomalous chemical trend indeed occurs in the Co-based group. A full account of the experiments on $Zn_{1-x}Co_xSe$ will be given in a separate paper.

The weak intrinsic peak broadening observed in the TOF experiments also confirms our previous conclusion

that spin-orbit-coupling effects play only a marginal role in the Co-Co interaction and that the anisotropic terms in Eq. (5) can be neglected in most cases. On the other hand, not all our observations can be accounted for by a simple Hamiltonian in the form of Eq. (1). The $|1\rangle \rightarrow |2\rangle$ transition peak seen at higher temperatures was found to be centered at 15.9 ± 0.1 meV, which is 0.5 meV below the expected value of 16.4 meV (i.e., the double energy of the $|0\rangle \rightarrow |1\rangle$ transition). However, similar deviations from the Landé rule are known to occur both in EPR and in neutron scattering experiments on other systems,[28,37] and can be described by adding a biquadratic term to the isotropic interaction Hamiltonian, so that

$$\mathcal{H} = 2J' \mathbf{S}_i \cdot \mathbf{S}_j + 2J'' (\mathbf{S}_i \cdot \mathbf{S}_j)^2 . \quad (9)$$

Physically, the biquadratic term arises as a higher-order intrinsic effect in superexchange processes,[38,39] or through an interplay of normal exchange interaction and elastic effects.[28,37] In the case of $S_i = S_j = \frac{3}{2}$, Eq. (9) leads to the following energy intervals between the successive levels: $2J' + 13J''$, $4J' + 14J''$, and $6J' - 3J''$. For the two transition energies observed in our experiments we obtain $J'_{NN} = 3.84$ meV (44.5 K), and $J''_{NN} = 0.04$ meV (0.46 K). The ratio of $J''_{NN}/J'_{NN} \approx 0.01$ is of similar order as observed in Mn-doped MgO (~ 0.05, Ref. 37), and in $CsMg_{1-x}Mn_xBr_3$ (0.005, Ref. 28). A reliable determination of the parameter set J_{NN}, J'_{NN} for $Zn_{1-x}Co_xS$ would require additional studies of the $|2\rangle \rightarrow |3\rangle$ transition, which is expected to occur in the range 23–24.5 meV. Unfortunately, no conclusive studies of this transition can be done on polycrystalline samples because of the strong peak in the density of phonon states in the same energy region (see Fig. 5). The growth of large good-quality monocrystals will clearly help to resolve this problem, because in TAS experiments on single crystals one can eliminate the unwanted phonon scattering by carrying out measurements at appropriate points of the Brillouin zone.

V. CONCLUDING REMARKS

In summary, we have determined the antiferromagnetic exchange integral J_{NN} for $Zn_{1-x}Co_xS$ from direct measurements of the Co-Co pair transition energies by means of inelastic neutron scattering. Our data confirm that the exchange interactions in Co-based DMS can, to a very good approximation, be described by an isotropic spin Hamiltonian, despite the spin-orbit-coupling effects indicated by the g-factor value of the Co^{2+} ion. As in Mn-based II-VI DMS alloys, the nearest-neighbor coupling appears to be the dominant magnetic exchange force in $Zn_{1-x}Co_xS$, which is in qualitative agreement with the predictions of superexchange theory.[4,8] However, the very large value of J_{NN} in the Co-based group points to the need for further quantitative analysis in the framework of this theory.

Our work has demonstrated that the TOF technique, so far not used for investigating excitations of magnetic pairs, offers a convenient and efficient experimental tool for such purposes. Another new methodological aspect of this study was the use of samples prepared by sintering procedures. Because of the relative ease of their preparation, neutron scattering measurements on sintered specimens offer a major simplification for identifying new DMS systems, and for characterization of their basic magnetic properties.

ACKNOWLEDGMENTS

We are grateful to A. Furrer and J. Spalek for reading the manuscript, and to M. Cieplak, T. Dietl, B. T. Jonker, B. E. Larson, and A. Lewicki for valuable comments and illuminating discussions. This work was supported by National Science Foundation Grant No. DMR-8821-635.

*Permanent address: Centro de Fisica, Instituto Venezolano di Investigacione Cientificas, Caracas, Venezuela.

[1] *Diluted Magnetic Semiconductors*, Vol. 25 of *Semiconductors and Semimetals*, edited by J. K. Furdyna and J. Kossut (Academic, Boston, 1988).

[2] J. K. Furdyna, J. Appl. Phys. **64**, R29 (1988).

[3] The most complete lists of references to J measurements in Mn-based II-VI DMS alloys can be found in Ref. 2, or in R. R. Galazka, W. Dobrowolski, J. P. Lascaray, M. Nawrocki, A. Bruno, J. M. Broto, and J. C. Ousset, J. Magn. Magn. Mater. **72**, 174 (1988).

[4] B. E. Larson, K. C. Hass, H. Ehrenreich, and A. E. Carlsson, Phys. Rev. B **37**, 4137 (1988); also Solid State Commun. **56**, 347 (1985).

[5] For a review of IV-VI DMS alloys, see G. Bauer, in *Diluted Magnetic (Semimagnetic) Semiconductors*, edited by R. L. Aggarwal, J. K. Furdyna, and S. von Molnar (Material Research Society, Pittsburgh, 1987), Vol. 89, p. 107. Studies of II-V DMS alloys have been reported by C. M. J. Denissen, H. Nishihara, J. C. van Gool, and W. J. M. de Jonge, Phys. Rev. B **33**, 7637 (1986), and C. M. J. Denissen, Sun Dakun, K. Kopinga, W. J. M. de Jonge, H. Nishihara, T. Sakakibara, and T. Goto, *ibid.* **36**, 5316 (1987).

[6] See, e.g., A. Bruno, J. P. Lascaray, M. Averous, G. Fillion, and J. S. Dumas, Phys. Rev. B **37**, 1186 (1988).

[7] All II-VI compounds have stable tetrahedral (i.e., zinc-blende or wurtzite type) crystallographic phases, except for HgS, which is stable only in cinnabar form; the exchange interactions in metastable zinc-blende $Hg_{1-x}Mn_xS$ have not yet been studied.

[8] K. C. Hass and H. Ehrenreich, J. Cryst. Growth **86**, 8 (1988).

[9] See, e.g., A. Mycielski, J. Appl. Phys. **63**, 3278 (1988).

[10] A. Twardowski, A. Lewicki, M. Arciszewska, W. J. M. de Jonge, H. J. M. Swagten, and M. Demianiuk, Phys. Rev. B **38**, 10749 (1988); H. J. M. Swagten, A. Twardowski, W. J. M. de Jonge, and M. Demianiuk, *ibid.* **39**, 2568 (1989).

[11(a)] B. T. Jonker, J. J. Krebs, and G. A. Prinz, Appl. Phys. Lett. **53**, 450 (1988); see also J. J. Krebs, B. T. Jonker, and G. A. Prinz, IEEE Trans. Magn. **24**, 2548 (1988), and B. T. Jonker, J. J. Krebs, G. A. Prinz, X. Liu, A. Petrou, and L. Salamanca-Young, in *Growth, Characterization, and Properties of Ultrathin Magnetic Films and Multilayers*, edited by B.

T. Jonker, E. E. Merinero, and J. P. Hermens (Material Research Society Symposium Proceedings, Pittsburgh, in press), Vol. 151.

[11(b)]D. U. Bartholomew, E.-K. Suh, A. K. Ramdas, S. Rodriguez, U. Debska, and J. K. Furdyna, Phys. Rev. B **39**, 5865 (1989).

[12]A. Lewicki, A. I. Schindler, J. K. Furdyna, and W. Giriat, Phys. Rev. B **40**, 2379 (1989).

[13]T. M. Giebultowicz, J. J. Rhyne, and J. K. Furdyna, J. Appl. Phys. **61**, 3537 (1987).

[14]H. A. Weakliem, J. Chem. Phys. **36**, 2117 (1962).

[15]F. S. Ham, G. W. Ludwig, G. D. Watkins, and H. H. Woodbury, Phys. Rev. Lett. **5**, 468 (1960).

[16]J. Kanamori, in *Magnetism*, edited by G. T. Rado and H. Suhl (Academic, New York, 1963), Vol. 1, p. 161.

[17]See, e.g., R. M. White, *Quantum Theory of Magnetism* (McGraw-Hill, New York, 1970).

[18]A. Stebler, H. U. Gudel, A. Furrer, and J. K. Kjems, Inorg. Chem. **21**, 380 (1982); B. Leuenberger, B. Briat, J. C. Canit, A. Furrer, P. Fisher, and H. U. Gudel, *ibid.* **25**, 2930 (1986); B. Leuenberger, H. U. Gudel, and A. Furrer, Chem. Phys. Lett. **126**, 255 (1986).

[19]W. L. J. Buyers, T. M. Holden, E. C. Swensson, and D. J. Lockwood, Phys. Rev. B **30**, 6521 (1984).

[20]J. Owen and E. A. Harris, in *Electron Paramagnetic Resonance*, edited by S. Geschwind (Plenum, New York, 1972), p. 427.

[21]B. R. Judd, *Operator Techniques in Atomic Spectroscopy* (McGraw-Hill, New York, 1963).

[22]See, e.g., J. M. Baranowski, J. W. Allen, and G. L. Pearson, Phys. Rev. **160**, 627 (1967), and references therein.

[23]V. Vagner and A. Furrer, Verh. Dtsch. Phys. Ges. **3**, 282 (1981).

[24]R. R. Galazka, S. Nagata, and P. H. Keesom, Phys. Rev. B **22**, 3344 (1980).

[25]Y. Shapira, S. Foner, D. H. Ridgley, K. Dwight, and A. Wold, Phys. Rev. B **30**, 4021 (1984); Y. Shapira, S. Foner, P. Becla, D. N. Domingues, M. N. Naughton, and J. S. Brooks, *ibid.* **33**, 356 (1986); R. L. Aggarwal, S. N. Jasperson, P. Becla, and R. R. Galązka, *ibid.* **32**, 5132 (1985).

[26]A. Furrer and H. U. Gudel, J. Magn. Magn. Mater. **14**, 256 (1979).

[27]E. C. Svensson, M. Harvey, W. L. J. Buyers, and T. M. Holden, J. Appl. Phys. **49**, 2150 (1970).

[28]U. Falk, A. Furrer, J. K. Kjems, and H. U. Gudel, Phys. Rev. Lett. **52**, 1336 (1984).

[29]L. M. Corliss, J. M. Hastings, S. M. Shapiro, Y. Shapira, and P. Becla, Phys. Rev. B **33**, 608 (1986).

[30]H. U. Gudel, A. Stebler, and A. Furrer, Inorg. Chem. **18**, 1021 (1979); H. U. Gudel and A. Furrer, Mol. Phys. **33**, 1335 (1977).

[31]B. E. Larson, K. C. Hass, and R. L. Aggarwal, Phys. Rev. B **33**, 1789 (1986).

[32]E. J. Lisher and J. B. Forsyth, Acta Crystallogr. Sect. A **27**, 545 (1971).

[33]K. Kunc, M. Balkanski, and M. A. Nusimovici, Phys. Status Solidi B **72**, 229 (1975).

[34]A. Lewicki, J. Spalek, J. K. Furdyna, and R. R. Galazka, Phys. Rev. B **37**, 1860 (1988).

[35]D. V. Bartholomew, E.-K. Suh, S. Rodriguez, A. K. Ramdas, and R. L. Aggarwal, Solid State Commun. **62**, 235 (1987).

[36]T. M. Giebultowicz, P. Klosowski, J. J. Rhyne, J. K. Furdyna, and U. Debska (unpublished).

[37]E. A. Harris and J. Owen, Phys. Rev. Lett. **11**, 9 (1963).

[38]P. W. Anderson, in *Solid State Physics*, edited by F. Seitz and D. Turnbull (Academic, New York, 1963), Vol. 14, p. 99.

[39]N. L. Huang and R. Orbach, Phys. Rev. Lett. **12**, 275 (1964).